

EXPERIMENTAL INSTRUMENTS AND TECHNIQUE

Analysis of Bolometer Operation near the Superconducting Transition Edge Using Microwave Readout

A. A. Kuzmin^a, S. V. Shitov^{b, c}, and A. V. Ustinov^c

^a Moscow Institute of Physics and Technology (State University),
Institutskii per. 9, Dolgoprudnyi, Moscow oblast, 141700 Russia

^b Kotel'nikov Institute of Radio Engineering and Electronics, Russian Academy of Sciences,
Mokhovaya ul. 17, Moscow, 125009 Russia

^c National University of Science and Technology MISiS, Leninskii pr. 4, Moscow, 119049 Russia

Received January 22, 2013

Abstract—The results of pioneering experiments on using a new method of microwave recording the bolometric response from a metal film near its superconducting transition edge are analyzed. Experiments are carried out at 4.5 K using a thin-film niobium absorber with a critical temperature of 6.7 K. The validity of the adopted electrodynamic model is confirmed. The chip contains a miniature antenna tuned to approximately 600 GHz and integrated into a planar resonator with a frequency of 6 GHz, which is weakly coupled with a pump line. Based on the experimental and model data, the presence of electrothermal feedback is shown, stability criteria are found, and I – V characteristics at microwaves are obtained. Bulk experimental samples with an absorber measuring $5\ \mu\text{m} \times 2.5\ \mu\text{m} \times 15\ \text{nm}$ are fabricated with optical photolithography. At an amplifier channel noise of 3 K, the optical sensitivity of a prototype receiver can be expected at a level of $10^{-15}\ \text{W/Hz}^{1/2}$.

DOI: 10.1134/S1063784214010101

INTRODUCTION

A new approach to the design of transition edge sensor (TES) bolometric detectors intended for array applications was theoretically substantiated in [1]. This approach consists in controlling the Q factor of a coupled resonator by varying its ohmic losses. It was shown that microwave heating of a nanodimensional titanium film inserted in a coupled resonator causes the film to pass from the superconducting state to the normal one. Using this method, one can make a detector with a sensitivity of about $10^{-19}\ \text{W/Hz}^{1/2}$ at a physical temperature of the sensor of about 300 mK. Experimental verification of the approaches described in [1] and elaboration of the experimental methods were started with a higher, liquid helium, temperature. Thin niobium films (Nb , $t_1 = 10$ – $30\ \text{nm}$), the critical temperature of which drastically varies with thickness, were used as a sensitive element. This allowed us to produce an all-niobium resonant structure. The superconducting transition temperature of this film, T_{c1} , may equal 5–7 K, and the film itself may serve as an absorber playing the role of a sensitive thermoresistor. At the same time, a resonator made of a thick niobium film ($t_2 = 200$ – $300\ \text{nm}$, $T_{c2} = 8$ – $9\ \text{K}$) is in the superconducting state and retains a high Q factor in the vicinity of the superconducting transition (near T_{c1}). In this paper, we analyze early experimental results [2, 3] obtained in terms of a new concept of bolometric response readout. The fabrication of experimental samples is described, as well as their dc testing and testing at a pumping current with a frequency of about 6 GHz.

PROTOTYPE DEVICE

The new concept is based on the design of a resonator shown in Fig. 1. A coplanar resonator excited at its eigenfrequency of about 6 GHz has a terahertz antenna into which a superconductor absorbing film near the superconducting transition is inserted. The antenna is intended for receiving terahertz signals and is matched to the absorber in the frequency range

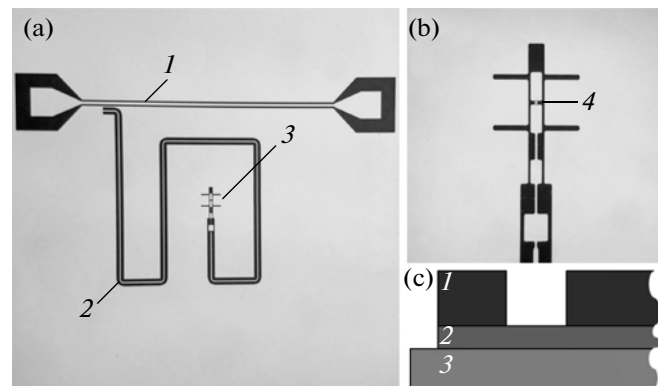


Fig. 1. Schematic of the experimental bolometer with microwave readout. (a) General view of the structure: (1) coplanar pumping line, (2) coplanar quarter-wave resonator, (3) 600-GHz slot antenna; (b) (4) open end of the resonator with the antenna and TES; and (c) layers of the structure: (1) thick niobium film of the coplanar resonator, (2) thin niobium film of the TES, and (3) sapphire substrate.

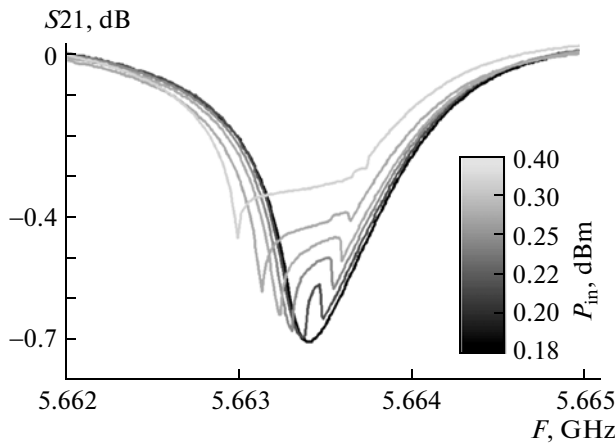


Fig. 2. Frequency dependence of the transmission of the pumping line with the TES-terminated Nb resonator at 5 K. Stepwise switching to the resistive state takes place at nearly the same microwave current passing through the TES. The lower curve corresponds to the superconducting state of the absorber in the resonator with $Q \approx 7000$.

620–670 GHz. Regardless of whether a signal is received or not, the current of the resonator passes through the absorber, heating it and keeping the film near the superconducting transition. Therefore, we will call the resonator-exciting current the pump current. Therein lies the main difference from standard TES bolometers, which approach the transition owing to the temperature of the cryostat (bath). The receiving array can contain a single transmission line equipped with a set of resonators similar to one shown in Fig. 1. If the frequencies of such high- Q resonators are slightly different (but their bands do not overlap), there appears the possibility of frequency selection of responses from different pixels with the line serving as a probe antenna akin to a multifrequency radar station. The comb spectrum generator of such a station must be tuned so that pumping at the frequency of each resonator heats up the thermoresistor to the working state in which the slope of the dependence $R(T)$ is optimum (maximum). In this case, a response to terahertz radiation is due to additional heating of the absorber and it is read out with a microwave amplifier at specific a priori known frequencies of the generator's comb spectrum. In our experiment with a single resonator, this takes place at a frequency of about 6 GHz in the form of variations of the pump signal traveling through the common line (Fig. 2). The structure contains a coplanar pumping waveguide ($Z_0 = 50 \Omega$) and a quarter-wave resonator ($Z_0 = 71 \Omega$) tuned to a frequency of about 5.6634 GHz. The geometry of the area where the pumping line is connected to the resonator was so selected that the frequency band of the unloaded resonator was 0.5 MHz. The correct choice of the electrodynamic parameters and their experimental implementation are confirmed by the experimental data shown in Fig. 2. The aim of the experi-

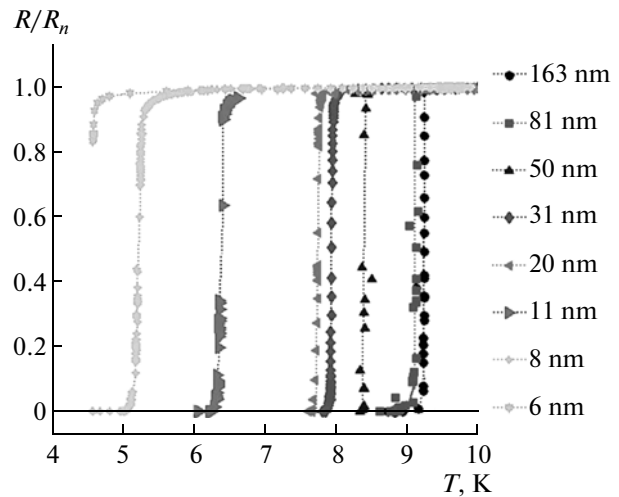


Fig. 3. Temperature dependences of normalized resistance $R(T)/R_n$ for test niobium films with decreasing thickness.

ment was to check microwave properties that were expected to show up at temperatures of about 4 K. The chip (Fig. 1a) was mounted on the flat surface of a semispherical sapphire lens by means of cyanoacrylate cement. The contact pads of the pumping line were welded with aluminum wires 20 μm thick to a special plate, which served as an electrical interface between the chip and leading-in coaxial cables. The entire assembly was fixed to a special holder and dipped in a transport Dewar vessel with liquid helium. During measurements, the device (chip) was in helium vapor at a temperature higher than 4.5 K rather than in liquid helium. The frequency characteristics were measured with an Agilent PNA-X circuit analyzer with an input signal power varying from -27 to $+6$ dBm.

FABRICATION OF TRANSITION EDGE SENSOR BOLOMETERS

To fabricate experimental micrometer-size transition edge sensor (TES) bolometers integrated with the antenna (Fig. 1), niobium films were magnetron-sputtered on a sapphire substrate ($\epsilon = 9.8$, $\tan\delta = 10^{-5}$). The resonator and antenna were made of a 200-nm-thick niobium film with critical temperature $T_c = 8.8$ K, and the absorber was prepared of niobium films with a thickness chosen from the range 10–20 nm so that the critical temperature of the superconducting transition was $T_c = 6.7$ K. To this end, we studied the suppression of T_c in reference films of different thickness [4] sputtered under the same conditions. The result of the controlled variation of the critical temperature in niobium films intended for the TES absorber is shown in Fig. 3.

The niobium films were deposited in a UNIVEX 450 magnetron sputterer with a deposition rate of 0.27 nm/s. The sputtering process was optimized for the argon pressure: the best films (maximum T_c and a

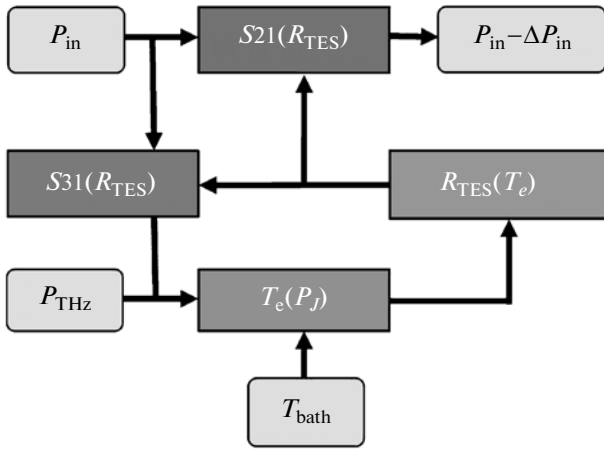


Fig. 4. Schematic diagram of the model used to simulate the device operation in the MATLAB-Simulink™ environment. Subsystems $S21(R_{TES})$ and $S31(R_{TES})$ were obtained by electromagnetic simulation of a chip including a pumping line, an antenna, and a resonator. Subsystems $R_{TES}(T_e)$ and $T_e(P_j)$ are the parameters of the absorber.

maximum relative resistance drop upon cooling) were deposited at a pressure of 5×10^{-3} mbar. The dc superconducting and transport properties of the films were studied using a measuring inset placed in the transport Dewar vessel filled with liquid He^4 (measurements were taken without temperature stabilization). A prototype of the microwave bolometer was fabricated by means of contact lithography. First, the sapphire substrate was covered by a thin (10–20 nm) niobium film intended for the absorber; then, a coplanar resonator, an antenna, and a pumping line were formed in the second 200-nm-thick Nb film by means of liftoff process. To provide a “clean” electrical contact between the niobium layers, the lower one was ion-cleaned using an argon gun before the deposition of the second layer. An absorber measuring $5 \mu m \times 2.5 \mu m \times 15 nm$ was etched out in the lower niobium layer by an Ar^+ ion beam with a photoresist in the absorber area and the second thick niobium layer over the remaining area of the chip used as a mask. The dc parameters of the absorber films were estimated indirectly using a witness sample with the same geometry of the absorber. The matter is that dc connection to the absorber in the resonator is impossible.

SIMULATION

The experimental data (Fig. 2) show that when the pumping power grows and reaches some threshold value, the response exhibits a singularity near the resonance frequency. It can be treated as switching to the low Q factor mode, which sets in after the (critical) current reaches a maximum in the resonator. Such behavior of the device is favorable for the photon count mode but is unfavorable when a linear-response bolometer is applied.

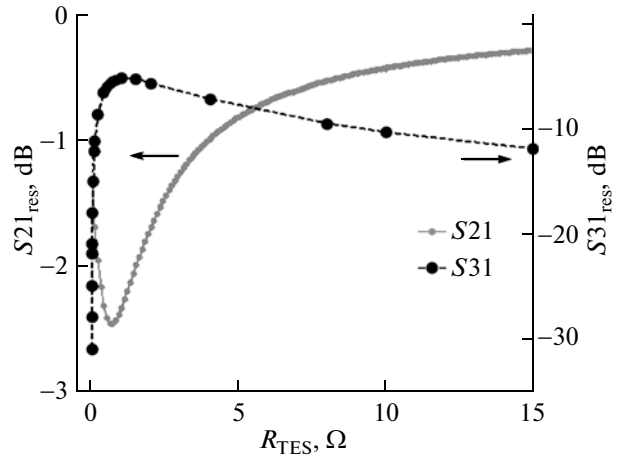


Fig. 5. Distributions of fixed pumping power P_{in} applied to the chip vs. resistance R_{TES} of the absorber in the resonator obtained by electromagnetic simulation. The curves are plotted in the form of scattering parameters (in dB).

To study the operating modes of the bolometer and, in particular, to find ways of how to bring the bolometer to the working point and estimate its sensitivity, numerical quasi-static simulation in the MATLAB-Simulink™ environment was performed using the device model shown in Fig. 4. The model allows one to obtain a numerical solution for the temperature and resistance of the absorber, as well as to estimate the device’s response to an external terahertz signal at any preset pumping power and bath temperature. The model of the device consists of four subsystems including linear electrodynamic scattering parameters $S21(R_{TES})$ and $S31(R_{TES})$ and also the dependences of heat exchange $R_{TES}(T_e)$ and $T_e(P_j)$ for three external parameters P_{in} , T_{bath} , and P_{THz} . Subsystems $S21(R_{TES})$ and $S31(R_{TES})$ describe the system’s response to a change in the mean value of the absorber resistance in the resonator.

The distribution of the microwave power in the “pumping line–variable- Q resonator” system can be found through the electromagnetic simulation of the structure shown in Fig. 1. The distributions of fixed pumping power P_{in} applied to the pumping line (chip) versus resistance R_{TES} of the absorber in the resonator is shown in Fig. 5 in the form of scattering parameters (in dB). Here, $S21$ is the coefficient of power transfer to the chip’s output port and $S31$ is the coefficient of (thermal) power P_j transfer to the absorber of the bolometer.

It is seen in Fig. 5 that at a low resistance, heating of the absorber (an increase in its resistance) leads to an increase in the released power; that is, positive feedback (PFB) takes place. After the resistance reaches some threshold value, further heating weakens absorption, which is equivalent to the presence of negative feedback (NFB).

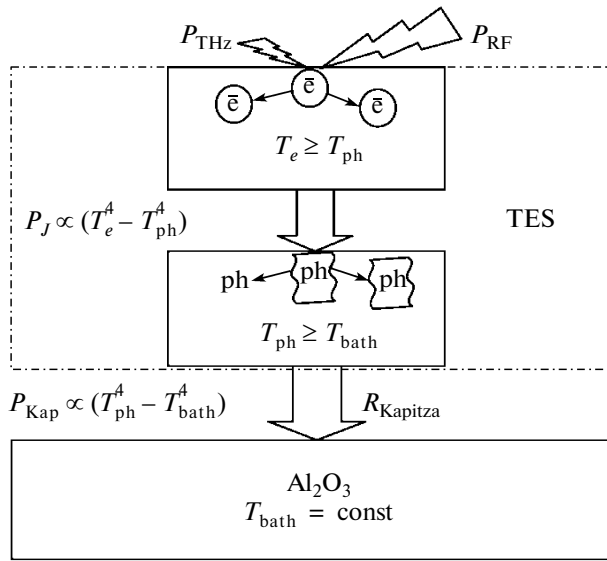


Fig. 6. Schematic representation of the absorber in the form of several interacting thermal subsystems. Since the time of electron–electron interaction is shorter than that of electron–phonon interaction at low temperatures, the temperature of the electron gas differs from that of the absorber array. At helium temperature, the Kapitza effect, which describes a temperature jump at the film–substrate interface, should also be taken into account.

Note that an attempt to switch the bolometer from the superconducting state to a finite-resistance state within the superconducting transition edge by varying the microwave power will almost inevitably end in failure. Due to positive feedback appearing at a low resistance, the absorber switches to the normal or back to the superconducting state not merely rapidly but in a self-accelerating (avalanche-like) manner. The absorber is heated or cooled by microwave current with the response speed (maximum speed) of the system, which causes instability. Thus, overheating proceeds in an avalanche-like manner similar to the superconducting–resistive switching of the film under the action of constant current. Moreover, from the analysis of the switching power it follows that the microwave current amplitude is almost equal to the switching current of the witness sample in dc measurements, i.e., to the film’s critical current. Pushing the analogy with dc measurements further, we notice that the current is less than critical and that exactly such currents correspond to the state within the superconducting transition and can be reached when moving down along the current hysteresis loop. In other words, they can be reached when the microwave power of our device, provided that it is already in the normal state, decreases. Such conditions were not realized in the above design of experiment, since frequency scanning was carried out at a constant pumping power.

Subsystems $R_{\text{TES}}(T_e)$ and $T_e(P_J)$ in the model shown in Fig. 4 are related to the absorber. Within the super-

conducting transition, resistance R_{TES} of the absorber strongly depends on its electron temperature T_e . When constructing the model, the dependence $R_{\text{TES}}(T_e)$ was derived from the dc experimental data for the witness sample. The absorber film was represented in the form of several interacting thermal subsystems (Fig. 6). Electron subsystem temperature T_e changes due to the absorption of microwave power coming from two sources: the resonator at a frequency of about 6 GHz and the terahertz antenna, $P_J = P_{\text{THz}} + P_{\text{RF}}$. The absorbed power is released as a heat flux through the phonon subsystem of the absorber into the sapphire substrate. Substrate temperature T_{bath} is kept constant. The time step of quasi-static simulation is limited from below by absorber time constant $\tau = C/G$ (C is the specific heat of the absorber, and G is the coefficient of thermal conduction from the absorber to the substrate). For the received signal (f_{THz}) and pumping signal (f_{res}), it is assumed that $f_{\text{res}} \gg 1/\tau$ and the absorber is so inert that it does not “sense” the alternating current phase. In other words, it is assumed that the absorber works as a square-law detector. If power P_J is applied to the absorber, the electron and phonon subsystems will take certain different temperatures within time τ . According to [5], these temperatures in thin Nb films are related to each other as

$$P_J = \nu \Sigma (T_e^4 - T_{\text{ph}}^4). \quad (1)$$

Here, $\nu \approx 0.2 \mu\text{m}^3$ is the absorber’s volume, $\Sigma = 8.2 \times 10^9 \text{ W}/(\mu\text{m}^3 \text{ K}^4)$ is a material parameter [5], T_{ph} is the phonon temperature, and T_e is the temperature of heated electron gas. Expression (1) is directly related to the temperature dependence of the time of electron–phonon interaction. For thin niobium films, it has the form $\tau_{\text{e-ph}} \propto T^2$. Theoretical consideration of the temperature dependence of $\tau_{\text{e-ph}}$ in thin disordered films is a challenging problem. To date, the dependence $\tau_{\text{e-ph}} \propto T^2$ for niobium films has not been fully understood and it is found experimentally. According to [6], at 4.5 K, $\tau_{\text{e-ph}} \approx 1 \text{ ns}$ and electron diffusion coefficient $D \approx 1 \text{ cm}^2/\text{s}$. Thus, the condition $f_{\text{res}} \gg 1/\tau$ is satisfied. Since the absorber is much longer than the diffusion length of electrons ($D\tau_{\text{e-ph}})^{1/2}$, the influence of heat removal into contacts can be neglected. The contribution of the thermal conductivity of the film–substrate interface (Kapitza resistance) to the time constant is usually neglected, since it is assumed to be much higher than $G_{\text{e-ph}}$. Heat flux P_{Kap} through the interface is given by

$$P_{\text{Kap}} = \sigma A (T_{\text{ph}}^4 - T_{\text{bath}}^4). \quad (2)$$

Here, $A \approx 12.5 \mu\text{m}^2$ is the contact area between the absorber and substrate and $\sigma \approx 5 \times 10^{-10} \text{ W}/(\mu\text{m}^2 \text{ K}^4)$ is a constant characterizing the niobium–sapphire interface. This constant can be roughly determined from the models of acoustic impedance mismatch and diffusion model [7]. It is seen that even if the small thickness of the film (effective two-dimensionality of

the phonon subsystem) is not taken into account, the contribution from the Kapitza resistance is not higher than 20%. Obviously, the condition $P_j \approx P_{\text{Kap}}$ should be satisfied under dynamic equilibrium.

For the model of the device constructed in the Simulink™ environment, time simulation was carried out at different external parameters P_{in} , T_{bath} , and P_{THz} . First, a way of bringing the TES bolometer to the working point with its intermediate resistance was investigated. In accordance with the results of electromagnetic simulation (see Fig. 4) and experimental data, the $S_{21}(R_{\text{TES}})$ and $R_{\text{TES}}(T_c)$ curves have a maximal steepness and $S_{31}(R_{\text{TES}})$ is expected to provide pumping power (P_{in}) negative feedback in the resistance range $R_{\text{TES}} = 1\text{--}5 \Omega$. To find a self-consistent solution, it is reasonable to choose the initial value of parameters for the working point (zero approximation) exactly in the resistance range where negative feedback takes place. The simulation result is shown in Fig. 7 in the form of the time dependences of P_{in} , T_{bath} , and R_{TES} .

A virtual experiment starts with cooling: the pumping power is not applied to the chip and the temperature was smoothly decreased from 9 to 4.2 K (Fig. 7, line 1). It is seen that the absorber resistance drops to zero (line 2) in accordance with the experimental curve $R(T)$. When the base temperature is reached, an attempt is made to reach the working point (the working temperature of the absorber) by simply increasing the pumping power (line 3) to a value certainly higher than that corresponding to the equilibrium state within the transition range. However, since the film is in the superconducting state, the microwave pumping power is almost not absorbed (S_{31} is negligibly small). Obviously, heating is impossible without the transition to the normal state, so that the absorber will remain in the superconducting state (line 2) until the microwave power reaches a level corresponding to the film's critical current.

The transition of the film to the resistive state by varying the bath temperature seems unreasonable, since this process is inertial. Inertia is fraught with a high probability of hysteresis loop formation and transition to the superconducting state. Variation of the pumping power is also a challenge, since possible random deviations during the incremental variation of the power may also lead to hysteresis. We suggest an approach shown in Fig. 7 that assumes pulsed heating of the device from 4.2 K to a temperature above T_c of the absorber with the pumping power and bath temperature T_{bath} preset and stabilized. Such a procedure provides smooth travel along the hysteresis loop above the critical current followed by relaxation to the equilibrium resistance of the absorber within the superconducting transition range, as demonstrated by the tails of the lines (Fig. 7). The preset pumping power for a given temperature can be found by calculations using the experimental parameters of the film, as was shown above.

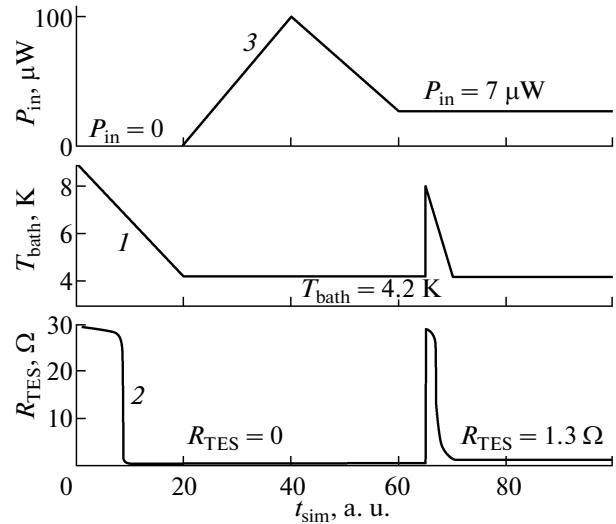


Fig. 7. Simulation of setting the TES absorber to the working point: (1) cooling down of the bath from 9 to 4.2 K at a zero pumping power, (2) superconducting transition in the absorber, (3) increase in the pumping power to a limiting (estimated) value with the aim of setting the absorber to an intermediate state with subsequent decrease to a minimum (estimated) power of stable operation, and (4) pulsed heating of the device above the critical temperature of the absorber.

When the working point is reached in our virtual experiment, we can investigate the dependence of R_{TES} on power P_j absorbed by the bolometer. To this end, expressions for the rms current and voltage across the absorber are applied,

$$\begin{cases} I_{\text{RF}} = \sqrt{P_j/R_{\text{TES}}} \\ V_{\text{RF}} = \sqrt{P_j R_{\text{TES}}}. \end{cases} \quad (3)$$

Based on expressions (3), a family of I – V characteristics of the absorber in the resonator $I_{\text{RF}}(V_{\text{RF}})$ was plotted for several temperatures of the bath (Fig. 8).

The I – V characteristics have the same form as the dc I – V characteristics of hot electron bolometer (HEB) mixers and conventional TES bolometers stabilized by electrothermal feedback [8, 9].

For the constructed model of the device (Fig. 4), one can estimate the watt–voltage sensitivity (S), amplification factor (G), saturation power (P_{sat}), and noise-equivalent power (NEP). In our virtual experiment, additional “test” thermal power was applied to the absorber, which was associated with signal ΔP_{THz} received by the terahertz antenna. Then, change ΔP_{in} in the output power of the pumping line was calculated. In the system with the TES bolometer, the power amplification factor was found to be $G = \Delta P_{\text{in}}/\Delta P_{\text{THz}} \approx 6.5$. Differentiating the relationship between the voltage and power in a matched pumping

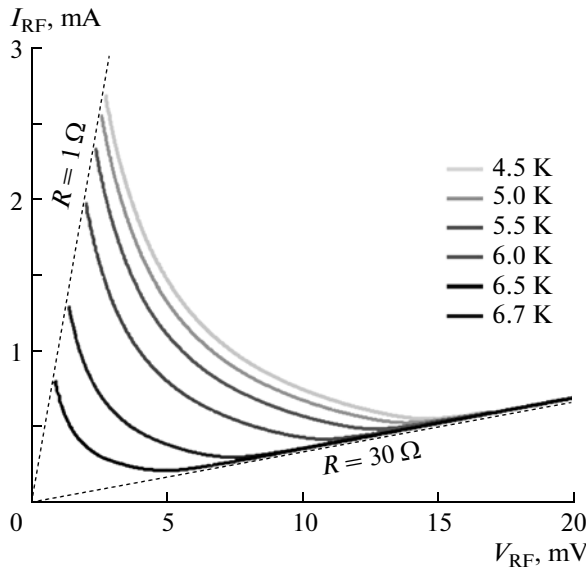


Fig. 8. Calculated I – V characteristics of the absorber in the resonator. Each point on the curves is a self-consistent solution for the dependence $P_J(R_{\text{TES}}(T_e|P_J, T_{\text{bath}}))$ at different temperatures T_{bath} of the bath and powers P_J absorbed by the absorber. The negative slope of the curves at low voltages indicates that the resonator serves as a “source of constant voltage” for the absorber and thereby provides the stabilization of the TES by means of negative electrothermal feedback.

line ($Z_0 = 50 \Omega$), we obtain the voltage modulation amplitude at the output of the device,

$$\Delta U_{\text{in}} = \frac{\Delta P_{\text{in}} Z_0}{2\sqrt{P_{\text{in}} Z_0}}. \quad (4)$$

From (4), one can find watt–voltage sensitivity $S = \Delta U_{\text{in}}/\Delta P_{\text{THz}} \approx 23000 \text{ V/W}$. If a cold semiconductor amplifier with noise temperature $T_N \approx 3 \text{ K}$ [10] below physical temperature $T_{\text{bath}} = 4.5 \text{ K}$ is placed at the output of the device, one can assume that thermal noise prevails. Having calculated the noise power of the amplifier in a 1 Hz wide band, we find that $\Delta U_{\text{noise}} \approx 9 \times 10^{-11} \text{ V/Hz}^{1/2}$ and $\text{NEP} = \Delta U_{\text{noise}}/S \approx 4 \times 10^{-15} \text{ W/Hz}^{1/2}$. This value of the NEP can be regarded as good for the rather bulk (micrometer-sized) device operating at helium temperature. The saturation power, which was defined as the thermal signal power at which the resistance of the bolometer becomes roughly equal to normal resistance $R_{\text{TES}} \approx 0.9R_N$, was $P_{\text{sat}} \approx 7 \mu\text{W}$.

CONCLUSIONS

It follows from the above analysis that the new device is really a variant of a TES bolometer using self-heating by a pumping current in the gigahertz frequency range. With the parameters of the electrodynamic system including a high- Q superconducting resonator chosen properly, the device can operate under the conditions of electrothermal negative feedback. This provides stabilization at a given working point within the range of the superconducting phase transition in a film along with a maximal sensitivity to external thermal and microwave electric signals including terahertz signals.

ACKNOWLEDGMENTS

The work was supported by the Russian Foundation for Basic Research (project no. 12-02-01352-a) and the Ministry of Education and Science of the Russian Federation (project nos. 11.G34.31.0062 and 11.G34.31.0029).

REFERENCES

1. S. V. Shitov, *Tech. Phys. Lett.* **37**, 932 (2011).
2. A. A. Kuzmin, S. V. Shitov, K. S. Il'in, J. M. Meckbach, S. Wuensch, M. Siegel, and A. V. Ustinov, *IEEE Trans. Terahertz Sci. Tech.* (2013).
3. A. A. Kuzmin, S. V. Shitov, K. S. Il'in, J. M. Meckbach, S. Wuensch, M. Siegel, and A. V. Ustinov, in *Proceedings of the 2nd International Conference “Terahertz and Microwave Radiation: Generation, Detection, and Applications” (TERA'2012), Moscow, 2012*, p. 52.
4. S. I. Park and T. H. Geballe, *Physica B & C* **135**, 108 (1985).
5. E. M. Gershenson, M. E. Gershenson, G. N. Gol'tsman, A. M. Lyul'kin, A. D. Semenov, and A. V. Sergeev, *Sov. Phys. JETP* **70**, 505 (1990).
6. E. T. Swartz and R. O. Pohl, *Rev. Mod. Phys.* **61**, 605 (1989).
7. P. J. Burke, R. J. Schoelkopf, D. E. Prober, A. Skalare, B. S. Karasik, M. C. Gaidis, W. R. McGrath, B. Bumble, and H. G. LeDuc, *J. Appl. Phys.* **85**, 1644 (1999).
8. E. M. Gershenson, G. N. Goltsman, I. G. Gogidze, Y. P. Gousev, A. I. Elantiev, B. S. Karasik, and A. D. Semenov, *Sov. Phys. Supercond.* **3**, 1582 (1990).
9. A. T. Lee, P. L. Richards, S. W. Nam, B. Cabrera, and K. D. Irwin, *Appl. Phys. Lett.* **69**, 1801 (1996).
10. N. Wadefalk, A. Mellberg, I. Angelov, et al., *IEEE Trans. Microwave Theory Tech.* **51**, 1705 (2003).

Translated by M. Astrov